9th Biennial International Conference
& Exposition on Petroleum Geophysics

"HYDERABAD 2012"

P-373

Subsurface Imaging: Through Multi-focusing Approach

Nikhil Agnihotri, Neeraj Tyagi, Shri A.K. Khanna, Dr R. Dasgupta*

Summary

Multi-focusing is regarded as homeo-morphic imaging, a one to one correspondence between the image and the real space. The core of the Multi- Focusing method is a new formula based on the ray pass theory, whose parameters are the radii of curvatures of different wavefronts, emergence angle, focusing parameter, and reference velocity. We review the multi-focusing method for travel time move out approximation of multi-coverage seismic data. Multi-focusing constructs the moveout based on two notional spherical waves at each source and receiver point, respectively. Time imaging provides sufficient information for a subsurface of moderate complexity. Moreover, even for complex areas that require depth migration for correct subsurface imaging, time imaging usually constitutes a key step that facilitates the estimation of a velocity model for depth imaging. Researchers attempt to avoid nonlinear stretch on short time intervals and distortions caused by a significant curvature of reflecting boundaries. Multi-focusing offers comprehensive accuracy of zero offset section since it relies on geometric considerations of the ray pass.

Keywords: *Multi-focusing, Subsurface Imaging, ERM*

Introduction

Multi-focusing stack is a latest method of zero-offset time imaging put forward by Boris Gelchinksy. We clarify the role of this focusing quantity which is a function of the source and receiver location, rather than a fixed parameter for a given multicoverage gather. The focusing function can be designed to make the traveltime moveout exact in certain generic cases that have practical importance in seismic processing and interpretation. The principle objective of multi-focusing is similar as for NMO-DMO stack: to create an accurate approximation of the zero-offset section with enhanced signal-to-noise ratio. In multi-focusing, this target is achieved by applying the move-out correction to large super-gathers comprising a large number of traces which need not belong to the same CMP gather, but whose sources and receivers are within a certain vicinity of the image point. Since the traces being stacked no longer belong to the same CMP gather, such a procedure requires a more general move-out correction than the one used in the conventional CMP stacking. Analytical expressions (based on the spherical representation of wave-fronts) describe the move-out correction for a given source-receiver pair with respect to a zero-offset image traced by three parameters measured at the image point. In Multi- focusing, the exact trajectory of arrivals is calculated for each sample without stretching of the wavelet, providing a much higher resolution especially in the shallow part of the section. In other words, the move- out correction expressed by the multi-focusing formulas is a three- parameter expansion of the travel time in the vicinity of the image point; accordingly it is closely related to the paraxial ray approximation (Tygel et al., 1997). The three parameters are: Emergence angle β, Radius of curvature of the wave- front of the Normal-Incidence-Point wave (NIP-wave radius R_{NIP}), Radius of curvature of the wave-front of the normal wave (N-wave radius R_N). All parameters being measured at the image point. The Normal-Incidence-Point (NIP) wave front is formed by a point source placed at the point where the zero- offset ray emitted from the image point hits the reflector (Fig. 1). The wave-front of the Normal (N) wave is formed by normal rays emitted by different points on the reflector (like in an "exploding reflector" model, Fig. 2).

NEF Project, Oil India Limited, Duliajan, Assam-786602, India
nikhil.agni@gmail.com

Exploding Reflector

Huygens principle states that wave motion can be described by exploding secondary sources along the wave front. The envelope of the resulting spheres constitutes successive wave fronts which progress in time. We have deviated slightly from Huygens principle, advocating that the explosions take place not along the wave fronts, but rather on the reflectors of the medium where the wave propagates whose magnitude is directly proportional to the reflection coefficient of that reflector. Each explosion point emits particles at each reflector point of the receivers yields the wave-fields. If the reflection coefficient vanishes, no additional explosion occurs at this point of time and space.

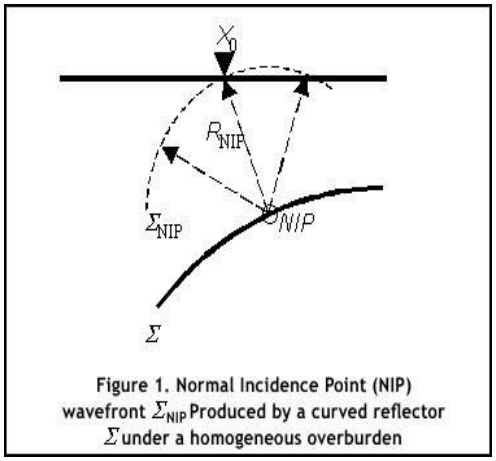

Figure 1. Normal Incidence Point (NIP) wavefront Σ_{NIP} Produced by a curved reflector Σ under a homogeneous overburden

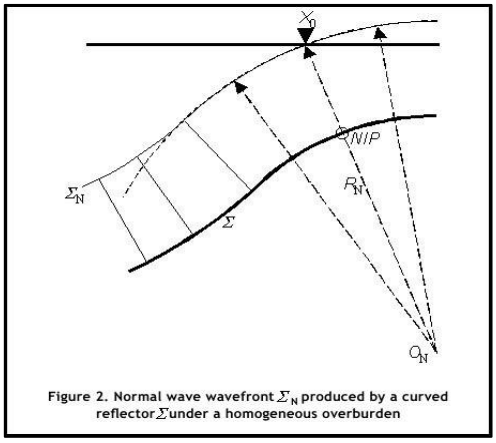

Figure 2. Normal wave wavefront Σ_N produced by a curved reflector Σ under a homogeneous overburden

Multi-focusing Parameters

The Multi-focusing parameters β, RN and RNIP have a clear physical interpretation, which allows a direct application in structural interpretation and velocity model building/inversion. The NIP wave, originating from a point source at a subsurface reflector, has a radius of curvature that depends on the propagation distance to the acquisition surface and hence on the depth of the reflector. For a single CMP gather the multi-focusing move-out correction reduces to the "shifted hyperbola" of de Bazelaire (1989), which is known to give a superior approximation of the travel time for a horizontally layered medium than the classical DIX NMO equation (Castle, 1994).

Multi-focusing Move-out Correction

The central ray starts at point X_0 with angle β to the vertical(refer to fig 3), hits the reflector ∑ at NIP and returns again at X_0. A paraxial ray from the source S intersects the central ray at point P and arrives back to the surface at point G. These two rays define a fictitious focusing wave which starts with the wave front $\sum_S$, focuses at P, is reflected at the reflector ∑ and emerges again at X_0 with the wave front $\sum_G$. Following the formulae of Gelchinsky et al. (1997), we can write the expression for move-out correction in the form

$$\Delta\tau = \frac{\sqrt{\left(R^+\right)^2 + 2R^+\Delta X^+ \sin\beta + \left(\Delta X^+\right)^2} - R^+}{V_0} + \frac{\sqrt{\left(R^-\right)^2 + 2R^-\Delta X^- \sin\beta + \left(\Delta X^-\right)^2} - R^-}{V_0} \quad \ldots\ldots\ldots\ldots\ldots\ldots (1)$$

Where,

$$R^{\pm} = \frac{1 \pm \sigma}{\frac{1}{R_{CEE}} \pm \frac{\sigma}{R_{CRE}}} \quad \ldots\ldots\ldots\ldots\ldots\ldots (2)$$

The quantity σ is related to the focusing of N and NIP Waves

$$\sigma = \frac{\Delta X^{+} - \Delta X^{-}}{\Delta X^{+} + \Delta X^{-} + 2\dfrac{\Delta X^{+}\Delta X^{-}}{R_{CRE}}\sin\beta};$$

Where ΔX^{+} and ΔX^{-} are the source and receiver offsets of an arbitrary ray with respect to the central ray, R^{+} and R^{-} are the wave front curvatures of the fictitious waves $\sum_S$ and $\sum_G$, respectively, and V_0 is the near surface velocity.

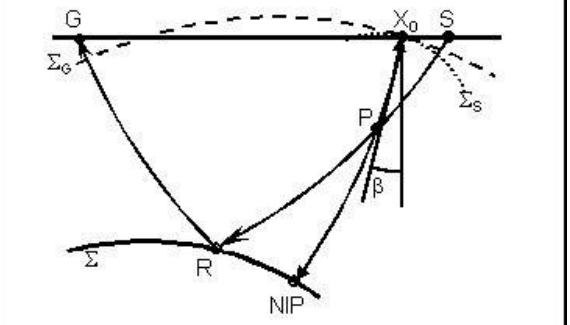

Figure 3: Ray diagram showing the construction of the focusing wave

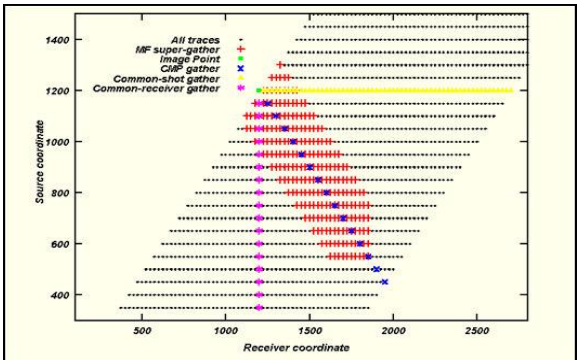

Figure 4. Multifocusing stacking chart in shot/receiver coordinates. The number of traces in a multifocusing super-gather (red crosses) is many times that in a CMP or common-shot, or common receiver gather

Quantities R^{+} and R^{-} involved in equation (1) are curvature radii of the fictitious wave fronts $\sum_S$ and $\sum_G$. It is clear from Fig.(3) that, for a given central ray, the radii R^{+} and R^{-} depend on the position of the source and receiver that define the paraxial ray (or, more precisely, on the position of the point P where paraxial ray intersects with the central ray). Equations (2) express the radii of the fictitious wave- fronts R^{+} and R^{-} through the fundamental curvature radii R_{NIP} and R_N, which are defined by the central ray only and are the same for all the source-receiver pairs in the vicinity of the central ray. The dependence of the radii R^{+} and R^{-} on the position of source and receiver (or on position of point P on the central ray) is contained in the focusing parameter σ which has a very clear physical interpretation. In particular, $\sigma = 0$ means that $R^{+} = R^{-} = R_N$, which implies that point P coincides with the radius of curvature of the normal wave (or of the reflector), and corresponds to the case of coinciding source and receiver (zero-offset configuration). The cases $\sigma = 1$ and $\sigma = -1$ imply $R^{-} = 0$ and $R^{+} = 0$, and correspond to the common – source and common-receiver configurations. The case $\sigma = \infty$ leads to $R^{+} = R^{-} = R_{NIP}$, and corresponds to the situation where the focusing point P coincides with NIP.

Move-out correction defined by equations (1)-(3) can be applied to arbitrary source and receiver offsets as long as the arcs of the fictitious wave fronts $\sum_S$ and $\sum_G$ can be considered spherical in shape.

The move-out correction in equation (1) is a sum of two hyperbolas. However, for all familiar source- receiver distributions this correction reduces to a single hyperbola. For a common source (common receiver) gather this can be readily seen after substituting $\Delta X^{+} = 0$ ($\Delta X^{-} = 0$) in equation (1). For a CMP gather which shows that for a single CMP gather and $R_N = \infty$ the multi-focusing move-out formula (1) reduces to the "shifted hyperbola" of de Bazelaire (1988), which is the most general practical NMO equation (Castle, 1994). The multi-focusing move-out correction as defined by equations (1)-(3) can be applied to any trace if its source and receiver are in some vicinity of the image point, for which we want to obtain the zero-offset trace. Thus, the multi- focusing move-out correction can be applied to large super-gathers without any loss of the spatial resolution. In multi-focusing, a super-gather is any set of traces whose sources and receivers are in

some vicinity of the image point. Examples of super-gathers are shown in Fig. 4

How Multi-focusing is better than other time imaging?

Advantage of multi-focusing over other traditional methods of time imaging (NMO+DMO) can be explained as follows: (1) Stacking a large number of traces belonging to different CMP gathers can increase signal-to-noise ratio by attenuating noise originating at a target depth. (2)For a flat reflector under a homogeneous overburden NIP radius depends on the distance between image point and the reflector and is independent of the reflector dip. For an inhomogeneous overburden R_{NIP} represents the distance between image point and the reflector in a reference medium (homogeneous medium with reference velocity V_0 equal to the velocity in the uppermost layer near the observation surface), again, independent of the dip. (3)Simultaneous determination of curvatures and emergence angle makes it possible to recover dip-independent RMS velocities V_{RMS} through a simple algebraic transformation,

$$V_{RMS} = \left(\frac{2V_0 R_{CRE}}{t_0} \right)^{1/2}$$

Where t_0 is the zero-offset arrival time at the image point; these velocities may be then used for migration. (4) The multi-focusing move-out correction for a given sample of the image trace at t_0 depends on the incidence angle and on curvatures measured on seismograms, and does not involve the value of t_0 itself. Thus all samples belonging to the same event would have the same parameters and hence the same move-out correction.

A Synthetic Example

(Courtesy: Ernesto G. Birgin etal, A New Algorithm for Traveltime Multiparameter Estimation, Department of Applied Mathematics-UNICAMP)

We consider the model of a single smooth reflector between two homogeneous acoustic half-spaces. Assuming unit density, the constant velocities above and below the reflector are v_1=2.5 km/s and v_2=2.6 km/s, respectively. The input data for our experiment is an ensemble of 61 common-shot (CS) and 61 common-mid-point seismic sections. Figure 5 shows the model and one of the common-shot experiments. The common-shot seismic sections have 30 traces each. The sources (x_0) lie in the range from 0 km to 0.6 km. The CMP seismic sections have 25 traces each, the mid points lying in the range from 0 km to 0.6 km. In both cases, the time window is 0:4s_t_9:1s. We have added a colored noise of 20%. This was obtained by the convolution of white noise with the wavelet used to construct the seismograms. Figures 6(a-c) show the theoretical and estimated parameters after the Initial Estimation Process.

Figures 6(d-f) show the theoretical and optimized parameters. Comparisons between theoretical and optimized parameters are depicted in Figures 6(g-i). Figure 7a,b show the semblance sections before and after the Optimization Process.

These sections can be looked upon as simulated zero- offset images of the reflector. They are called in Gelchinsky *et al.* (1997) semblancegrams. Finally, 7c shows the maximum semblance function values on the upper branch of the simulated zero-offset image of the reflector before and after the Optimization Process.

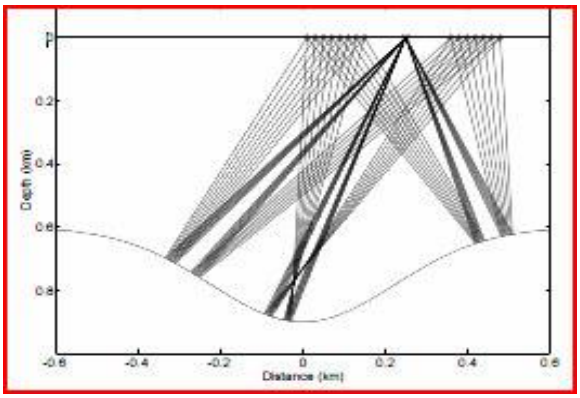

Figure 5: Model and CS acquisition Geometry

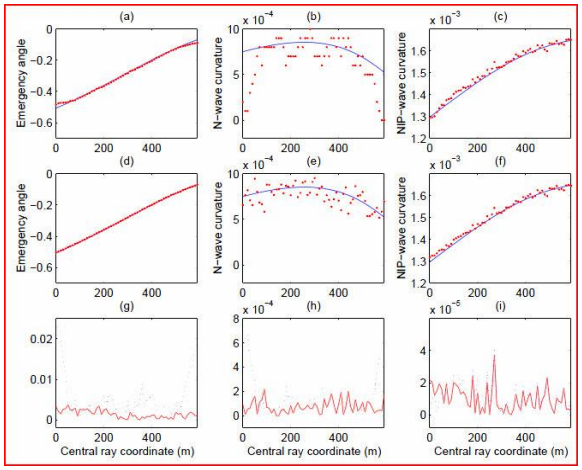

Figure 6: (a-c) theoretical (solid lines) and estimated (dots) parameters after one-dimensional searches. (d- f) theoretical (solid lines) and estimated (dots) parameters after optimization process. (g-i) absolute errors between theoretical and pre- (dots) and post-optimization (solid line) parameters.

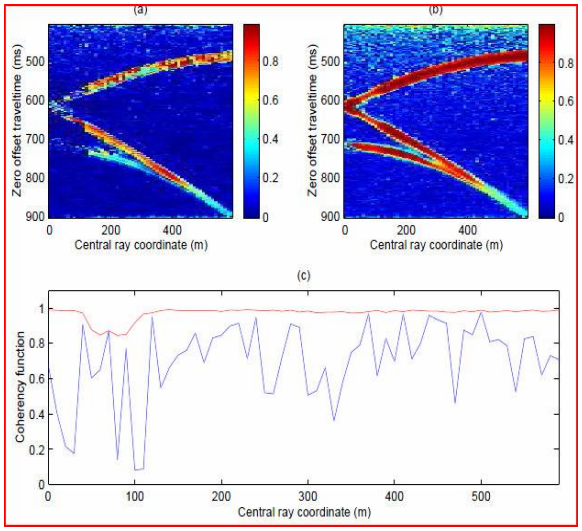

Figure 7: Coherency function evaluated on CS gathers. (a) before optimization, (b) after optimization, and (c) pre- and post-optimization over the reflector. See the great improvement in coherency fucntion value along the reflector.

Conclusion & Implementation

Indeed, implementation of the multi-focusing method has an inherent complexity i.e. How traveltime is parameterized by three imaging parameters: β, R_{NIP} and R_N instead of a single parameter i.e. stacking velocity in the conventional NMO stack? For NMO stack, the stacking velocity is usually determined by means of the interactive velocity analysis. For the multi-focusing parameters a similar procedure is out of the question for two reasons, (1) Due to huge cost involvement.

(2) Even if such computation was possible, an interactive procedure would have to involve displaying and picking of maxima of the correlation measure as a function of four variables (t0 and three imaging parameters), which does not look feasible. Thus, the determination of the imaging parameters must involve some kind of optimization methods.

This, in turn, brings about all sorts of problems associated with automatic correlation/stacking procedures, which have been encountered before in numerous attempts to construct an automatic NMO stack. Automatic procedures optimally stack useful signal as well as noise, especially spatially correlated noise e.g. strong multiples may have higher correlation measure than weaker signals via interactive correlation procedures this ambiguity could be addressed manually by picking right maxima on the basis of a priori velocity information. In the automatic procedure the only way is to impose constraints on the imaging parameters. Implementation of the multi-focusing method is based on a phase correlation of signal on the observed seismic traces. The data is move-out corrected along different travel time curves to find the curve closest to the travel time curve of the signal. The unknown parameters β, RNIP, and RN are estimated by finding a set of parameters which maximizes the semblance function calculated for all seismic traces in a chosen offset range around a central trace in a time window along the travel time curve defined by expression (1). Maximization of the semblance is achieved by a nonlinear global optimization method. The correlation procedure described above is repeated for each central image point as well as for each time sample forming a multi-focusing time section (MFS). Each sample on MFS represents the optimal stacked value corresponding to the optimal parameters of β, RNIP and RN and it is close to an accurate zero-offset section. Estimated sets of parameters can also be represented in the time section forming a so-called angle-gram β(x,t) and radius-grams RNIP(x,t0), RN(x,t0).

References

www.journalseek.net,
http://geo.gii.co.il,
www.geomage.com

Berkovitch A. , Belfer I. and Landa E. ,2008, Multifocusing as a method of improving subsurface imaging ,The Leading Edge; v. 27; no. 2; p. 250-256; DOI: 10.1190/1.2840374

Ernesto G. Birgin etal, A New Algorithm for Traveltime Multiparameter Estimation, Department of Applied Mathematics-UNICAMP

De Bazelaire, E., 1988, Normal moveout correction revisited: Inhomogeneous media and curved interfaces, Geophysics, 53, 143-157.

Berkovitch, A., Keydar, S., Landa, E., and Trachtman, P, 1998, Multifocusing in Practice, 68th Annual Meeting, Society of Exploration Geophysicists, Expanded Abstracts.

Castle, R., A theory of normal moveout, 1994, Geophysics, 59, 983-999.

Gelchinsky, B., Berkovitch, A., and Keydar, S., 1997, Multifocusing Homeomorphic Imaging: Part 1: Basic concepts and formulae: Presented at the special course on Homeomorphic Imaging by B. Gelchinsky, Seeheim, Germany.

Tygel, M., Muller, Th., Hubral, P., and Schleicher, J., 1997, Eigenwave based multiparameter traveltime expansions, 67th Annual Meeting, Society of Exploration Geophysicists, Expanded Abstracts, 1770-1773.

Acknowledgement

The authors are greatly thankful to Mr. K.K.Nath, ED (operations) for his constant support and encouragement while preparing this paper.

Views expressed in this paper are that of the author(s) only and may not necessarily be of OIL.